

# From pattern to process? Dual travelling waves, with contrasting propagation speeds, best describe a self-organised spatio-temporal pattern in population growth of a cyclic rodent

Deon Roos<sup>1</sup>, Constantino Caminero-Saldaña<sup>2</sup>, David Elston<sup>3</sup>, Francois Mougeot<sup>4</sup>, María García-Ariza<sup>2</sup>, Beatriz Arroyo<sup>4</sup>, Juan José Luque-Larena<sup>5</sup>, Francisco Rojo Revilla<sup>2</sup>, and Xavier Lambin<sup>1</sup>

<sup>1</sup>University of Aberdeen

<sup>2</sup>Instituto Tecnológico Agrario de Castilla-y-León (ITACyL)

<sup>3</sup>Biomathematics & Statistics Scotland

<sup>4</sup>Instituto de Investigación en Recursos Cinegéticos (IREC, CSIC-UCLM-JCCM)

<sup>5</sup>Universidad de Valladolid

February 22, 2024

## Abstract

The dynamics of cyclic populations distributed in space result from the relative strength of synchronising influences and the limited dispersal of destabilising factors (activators and inhibitors), known to cause multi-annual population cycles. However, while each of these have been well studied in isolation, there is limited empirical evidence about how the processes of synchronisation and activation-inhibition act together, largely owing to the scarcity of datasets with sufficient spatial and temporal scale. We assessed a variety of models that could be underlying the spatio-temporal pattern, designed to capture both theoretical and empirical understandings of travelling waves using large-scale (> 35,000 km<sup>2</sup>), multi-year (2011-2017) field monitoring data on abundances of common vole (*Microtus arvalis*), a cyclic agricultural rodent pest. We found most support for a pattern formed from the summation of two radial travelling waves with contrasting speeds that together describe population growth rates across the region.

## Title

From pattern to process? Dual travelling waves, with contrasting propagation speeds, best describe a self-organised spatio-temporal pattern in population growth of a cyclic rodent

## Running title

Dual travelling waves in population growth

## Authors

Deon Roos<sup>a,b</sup>, Constantino Caminero-Saldaña<sup>b</sup>, David Elston<sup>c</sup>, François Mougeot<sup>d</sup>, María Carmen García-Ariza<sup>b</sup>, Beatriz Arroyo<sup>d</sup>, Juan José Luque-Larena<sup>e,f</sup>, Francisco Javier Rojo Revilla<sup>b</sup>, Xavier Lambin<sup>a</sup>

1. School of Biological Sciences, University of Aberdeen, Tillydrone Avenue, Aberdeen, AB24 2TZ, UK
2. Área de Plagas, Instituto Tecnológico Agrario de Castilla-y-León (ITACyL), Ctra. Burgos km 119, 47071, Valladolid, Spain
3. Biomathematics & Statistics Scotland, Craigiebuckler, Aberdeen, AB15 8QH, UK

4. Instituto de Investigación en Recursos Cinegéticos, IREC (CSIC-UCLM-JCCM), Ronda de Toledo 12, 13071, Ciudad Real, Spain
5. Dpto. Ciencias Agroforestales, ETSIIAA, Universidad de Valladolid, Avda. de Madrid 44, 34004, Palencia, Spain
6. Instituto Universitario de Investigación en Gestión Forestal Sostenible, Palencia, Spain

### **CRedit Statement of authorship**

**Deon Roos** : Conceptualization, Methodology, Software, Validation, Formal analysis, Data Curation, Writing - Original Draft, Writing - Review & Editing, Visualization **Constantino Caminero-Saldaña** : Conceptualization, Methodology, Investigation, Resources, Data Curation, Writing - Review & Editing, Supervision, Project administration, Funding acquisition **David Elston** : Conceptualization, Methodology, Validation, Formal analysis, Writing - Review & Editing, Supervision **François Mougeot** : Conceptualization, Writing - Review & Editing, Supervision **María Carmen García-Ariza** : Methodology, Investigation, Data Curation **Beatriz Arroyo** : Conceptualization, Writing - Review & Editing, Supervision **Juan José Luque-Larena** : Conceptualization, Resources, Writing - Review & Editing, Supervision **Francisco Javier Rojo Revilla** : Methodology, Investigation, Data Curation **Xavier Lambin** : Conceptualization, Validation, Resources, Writing - Review & Editing, Supervision, Project administration, Funding acquisition

### **Data accessibility statement**

Should the manuscript be accepted, the data supporting the results will be archived in an appropriate public repository and the data DOI will be included at the end of the article.

### **Emails**

DR: [deonroos99@hotmail.com](mailto:deonroos99@hotmail.com), CSS: [camsalco@itacyl.es](mailto:camsalco@itacyl.es), DE: [David.Elston@bioss.ac.uk](mailto:David.Elston@bioss.ac.uk), FM: [Francois.Mougeot@uclm.es](mailto:Francois.Mougeot@uclm.es), MCG-A: [ita-gararima@itacyl.es](mailto:ita-gararima@itacyl.es), BA: [Beatriz.Arroyo@uclm.es](mailto:Beatriz.Arroyo@uclm.es), JLL-L: [j.luque@agro.uva.es](mailto:j.luque@agro.uva.es), RJRR: [rojrevfr@itacyl.es](mailto:rojrevfr@itacyl.es), XL: [x.lambin@abdn.ac.uk](mailto:x.lambin@abdn.ac.uk)

### **Further Ecology Letters information**

Type of article: Letter

Number of words in abstract: 145

Number of words in main text (excluding abstract and legends): 5031

Number of references: 79

Number of figures, tables, and text boxes: 2 tables + 3 figures (+ 1 video)

Corresponding author: Xavier Lambin, [x.lambin@abdn.ac.uk](mailto:x.lambin@abdn.ac.uk)

### **Abstract**

The dynamics of cyclic populations distributed in space result from the relative strength of synchronising influences and the limited dispersal of destabilising factors (activators and inhibitors), known to cause multi-annual population cycles. However, while each of these have been well studied in isolation, there is limited empirical evidence about how the processes of synchronisation and activation-inhibition act together, largely owing to the scarcity of datasets with sufficient spatial and temporal scale. We assessed a variety of models that could be underlying the spatio-temporal pattern, designed to capture both theoretical and empirical understandings of travelling waves using large-scale (> 35,000 km<sup>2</sup>), multi-year (2011-2017) field monitoring data on abundances of common vole (*Microtus arvalis*), a cyclic agricultural rodent pest. We found most support for a pattern formed from the summation of two radial travelling waves with contrasting speeds that together describe population growth rates across the region.

### **Keywords**

spatio-temporal | patterns | population cycles | population growth rate | synchrony

## Introduction

Classic ecological theory assumes that population dynamics result from interacting organisms in time but in a non-spatial context (e.g., Lotka-Volterra model). However, these predictions are modified when accounting for restricted species movement by including space and dispersal (Levin 1974). When interactions between pairs of species, broadly fitting the definition of activator-inhibitor (such as predator-prey, parasite-host, etc.), result in local cycles, incorporating space and accounting for restricted dispersal can give rise to spatio-temporal patterns (de Roos *et al.* 1991; Bjørnstad *et al.* 2002; Sherratt 2001; Johnson *et al.* 2006). These dynamic spatial patterns can take various forms, ranging from chaos (Liet *et al.* 2005) to perfect synchrony (Blasius *et al.* 1999) and much in between.

Causes of synchrony have been attributed to climate conditions (the Moran effect, e.g., Bogdziewicz *et al.* 2021), dispersal of individuals, and trophic interactions. While the Moran effect is often suggested as the cause of synchrony (e.g., Fay *et al.* 2020), microcosm experiments have strongly implicated an interaction between dispersal of organisms and their trophic interactions through the differential depletion of denser than average prey/host populations as a potent cause of synchrony (Vasseur & Fox, 2009; Fox *et al.* 2013).

Synchrony itself exists on a spectrum. Of note are periodic travelling waves (termed *partial synchrony* in Fig. 1B), whereby the oscillations of population cycles seemingly travel across space over time, either in a single constant direction (i.e., anisotropic, henceforth termed *planar wave*, e.g., Lambin *et al.* 1998; Berthier *et al.* 2014; Bjørnstad *et al.* 2002) or in all directions (i.e., isotropic; henceforth termed *radial wave*, e.g., Johnson *et al.* 2004), at a given speed. For population cycles linked via a travelling wave, all populations experience the same cycle, but do so at potentially different times. For such populations, with increasing distance between them, the cycle will become increasingly asynchronous until eventually returning to the same cycle phase. Conversely, a perfectly synchronised cycle (termed *true synchrony* in Fig. 1C) is merely one where the wave speed is practically infinite (Jepsen *et al.* 2016; Sherratt 2001). In a cycle with true synchrony, all populations in a landscape exhibit the same phase of the cycle simultaneously with no spatio-temporal lag. The opposing end of the synchrony spectrum would be populations that are disconnected and cycle completely independently of each other (termed *true asynchrony* in Fig. 1A).

While travelling waves appear to be routinely detected when datasets are sufficient, there remains much uncertainty. Namely, what form a travelling wave will take when spreading across a natural landscape, what features determine the source location(s) of the wave(s), and whether activator-inhibitor dynamics play a role in the underlying mechanisms generating travelling waves?

Theoretical simulations of travelling waves unfolding in homogenous landscapes suggest the spread should be radial. However, real world landscapes include habitat heterogeneity (but see Johnson *et al.* 2006). Intriguingly, spatial inhomogeneity can lead to the formation of both radial and planar waves via either variation in productivity, connectivity or interactions with dispersal. However, theoretical work explicitly investigating the role that heterogenous landscapes have on travelling waves, via inclusion of physical features (e.g. lakes), suggest that waves may originate from these structures with an imparted directionality (Sherratt *et al.* 2002; Sherratt *et al.* 2003). If the feature preventing isotropic dispersal is itself linear, then the resulting form of the wave would be expected to be planar. Because heterogeneities are ubiquitous in real landscapes and affect both dispersal and productivity, theory offers no prediction on what pattern should unfold in any real-world landscapes and arguments on any match between empirical pattern and theory have been post-hoc.

Empirical research projects, which by their nature occur in heterogenous environments, have often used planar wave parameterisations to describe the observed travelling waves in cyclic populations (Lambin *et al.* 1998; Berthier *et al.* 2014). Such a mismatch between generally predicted (i.e., radial) and observed (i.e., planar) patterns may have two interpretations. The first may be that the apparent planar waves are simply a feature of observing a radial wave at too small a spatial scale (feasible given the substantial data requirements [Koenig 1999]). Alternatively, observed planar waves may reflect real world conditions which

some simulations fail to account for (e.g. heterogenous landscapes with regards to the distribution of both habitats and organisms). Thus, true planar waves may arise due to approximately linear physical features in the landscape. Building on Sherratt and Smith's (2008) theoretical work, which suggested physical features may generate travelling waves, Berthier *et al.* (2014) invoked quasi-linear physical features in their landscape as being potentially responsible for planar waves in cyclic montane water vole populations. However, because of necessary theoretical assumptions for how physical features interact with organisms (resulting in boundary conditions which are hard to quantify empirically) Berthier *et al.* (2014) could not ascertain which of two plausible features were responsible. This reflects the challenge of translating theoretical assumptions into real-world characteristics and vice-versa.

An alternative to physical features generating travelling waves is the suggestion that they are generated in foci with particular features. Such features include: areas with high densities (Bulgrim *et al.* 1996); areas where predators were introduced (Sherratt *et al.* 1997; Gurney *et al.* 1998; Sherratt *et al.* 2000; Sherratt 2001; Sherratt 2016) and areas of high population connectivity or habitat quality (Johnson *et al.* 2006). The epicentre hypothesis posits that travelling waves recurrently form via epicentres. These epicentres reflect regions in space with defined characteristics (e.g., highly connected populations in high quality habitats) that give rise to waves. Johnson *et al.* (2006) invoked the epicentre hypothesis to explain travelling waves in cyclic larch bud moths (Johnson *et al.* 2004), whereby they proposed that waves emanate from regions with high-quality, well-connected populations which then spread to more distant populations, resulting in partially synchronous cycles.

Related to uncertainties with what generates a wave, is the ambiguity of theory on resulting direction of travel relative to the source. It has been suggested for the larch budmoth that waves travel outwards from epicentres (Johnson *et al.* 2006), resulting in expanding radial travelling waves. Conversely, alternative studies have suggested the opposite may occur, whereby waves begin at hostile environment boundaries (i.e. where individuals die if entered) and contract inwards towards a central location (Sherratt 2003; Sherratt & Smith 2008). There has been no empirical research with an analytical approach that explicitly tested for such expanding or contracting waves.

As a wave spreads, via dispersal and trophic interaction (Vasseur & Fox 2009), the cycle spreads across a landscape from one population to the next, each population in turn experiences the same cyclical successions of activation or inhibition of growth rates. Such changes to a population's growth rate are, in part, dependent on neighbouring populations. For instance, inhibition may represent the spread of agents such as pathogens or predators from one population to the next, resulting in local populations being suppressed as the respective wave passes. Theoretical expectations of travelling waves have been supported by empirical evidence from a variety of fields, all of which can be considered to have such activator-inhibitor relationships; e.g., herbivore-plant, predator-prey, parasite-host, (Lambin *et al.* 1998; Moss *et al.* 2000; Johnson *et al.* 2004; Bierman *et al.* 2006; Mackinnon *et al.* 2008; Berthier *et al.* 2014), susceptible-recovered, (Grenfell *et al.* 2001; Cummings *et al.* 2004), death and regeneration (Sprugel 1976), and cellular biochemistry (Müller *et al.* 1998; Bailles *et al.* 2019) amongst others. Within such systems, it is the cumulative impact of both activator and inhibitor that gives rise to the overall cyclic pattern.

The conceptualisation of population cycles as activation-inhibition, as well as the wealth of theoretical literature considering the role of such activation and inhibition accompanied by restricted dispersal in spatial patterns (Levin 1974; de Roos *et al.* 1991; Bjørnstad *et al.* 2002; Sherratt *et al.* 2000; Sherratt 2001; Johnson *et al.* 2006) implies that statistical representation of empirical data might decompose the overall pattern in growth and retrieve evidence of two contributing travelling waves, promoting and inhibiting growth, respectively, as found in non-ecological travelling waves (Kapustina *et al.* 2013; Martinet *et al.* 2017). Additionally, the interplay between dispersal abilities of activator and inhibitor have been suggested as a component which leads to the formation of radial and planar waves (Johnson *et al.* 2006).

Building on exceptional data, this study evaluates a suite of hypotheses, which are flexible phenomenological descriptions of travelling waves, representing theoretical or empirical work or their logical extensions. Given the richness of our dataset, we are able to lessen requirements for simplified caricatures and consider more

complex forms. Our approach considers an initial demarcation between radial and planar waves, including whether the radial waves contract or expand. These hypotheses are further divided to represent either a single travelling wave or multiple (as simulated in Johnson *et al.* 2006), each in turn split into whether multiple waves are isolated from each other by physical features or coalesce into a single pattern reflecting activator-inhibitor dynamics. To do so, we used abundance indices of a rodent crop pest from a study site spanning  $> 35,000 \text{ km}^2$  over seven years. We find evidence of a single cumulative spatio-temporal pattern consisting of two expanding radial travelling waves, which we propose may arise due to activator-inhibitor dynamics.

## Materials and Methods

### Study species

The common vole (*Microtus arvalis*) is a small rodent inhabiting natural grasslands and agricultural ecosystems in Europe. It is prey for both specialist and generalist predators alike (Mougeot *et al.* 2019) and is the host of multiple direct and vector transmitted pathogens (Rodríguez-Pastor *et al.* 2019). Common voles are a frequent farmland pest causing both crop damages and disease spillovers during population outbreaks that occur every 3-4 years (Jacob & Tkadlec 2010; Mougeot *et al.* 2019; Rodríguez-Pastor *et al.* 2019). Common voles have been extensively monitored for pest management across our study site ( $> 35,000 \text{ km}^2$ ) since 2011.

### Study site

We (ITACyL) collected data on vole abundances in Castilla-y-León (CyL), NW Spain. CyL is a large ( $94,226 \text{ km}^2$ ), relatively flat semi-arid agro-steppe plateau encircled by mountains and bisected east to west by the ca. 25-150 m wide Duero River (Fig. 2). As a result of land-use changes (ca. the 1970s), common voles colonised the plateau from the adjacent mountain ranges in the north, east and south (Luque-Larena *et al.* 2013, Jareño *et al.* 2015). Within the wider region, common voles are believed to occur at higher densities within the plateau than in the surrounding mountains, likely due to the region's agricultural practices (Roos *et al.* 2019). A particular area in the centre of CyL (*Tierra de Campos*) is known to practitioners as problematic due to early, large or persistent outbreaks.

While not a perfectly homogenous landscape, the plateau likely presents a "best real-world match" for conditions used in most theoretical research, which do not account for landscape features (but see Sherratt & Smith 2008). However, there are two complicating physical features: the Duero river and surrounding mountain ranges. If physical features are related to the form of a wave, we may expect either planar waves that travel north and south due to the river or a contracting radial wave resulting from the encircling mountains.

### Data collection

We made use of a widely employed calibrated abundance index method, based on vole presence, to monitor vole abundance at large spatial scales (Roos *et al.* 2019; Jareño *et al.* 2014). Transects, up to 99 m in length (dependent on the field's length), were carried out in linear stable landscape features (field, track or ditch margins) to estimate vole abundance from winter 2011 until autumn 2017 ( $n = 42,973$ ). Margins are known to be reservoir habitats for voles, where from voles colonise adjacent fields during outbreak periods (Rodríguez-Pastor *et al.* 2016). Each transect was divided into 3 m sections (33 in total), with each section noting the presence or absence of one or more signs of vole activity (i.e., latrines by burrows, fresh vegetation clippings, and recent burrow excavations). The proportion of sections with signs of vole presence per transect was then used as the abundance index. The number of surveys carried out at any time varied adaptively with the perceived risk of an outbreak (according to changes in estimated abundance in previous monitoring surveys).

Analyses of travelling waves typically use some measure that can detrend from long-term temporal trends and autocorrelation, such as phase angle or log difference growth rates (Liebhold *et al.* 2004; Vindstad *et al.* 2019). As such, the response variable typically used in all models is proportional growth rate ( $r_t =$

$\ln(N_{t+1}) - \ln(N_t)$ , where  $N$  is the abundance index at time  $t$  (Royama 1992; Berryman 2002). A benefit of using  $r_t$ , rather than  $\ln(N_t)$ , is that any multiplicative effects of site quality are cancelled out, provided they are constant over time. To calculate  $r_t$ , vole abundance indices are required at the same location in subsequent time periods (i.e.,  $t$  and  $t + 1$ ). To achieve this, transects were temporally aggregated into a respective yearly quarter (e.g., January to March 2014). Transects were then spatially aggregated by using an arbitrarily chosen transect as a reference point and assigning all transects within a 5 km radius to the  $i^{\text{th}}$  centroid, with any transect only assigned to a single centroid. Once complete, the mean Julian day, X and Y UTM (Universal Transverse Mercator) were calculated for each centroid.

We chose three-month intervals and 5 km centroids as these time periods and spatial scales maximised the number of centroids with successive abundance indices, increasing the number of growth rate estimates that could be calculated. A constant of 3.03 was added to  $N$  to avoid zero entries (3.03 was the lowest non-zero value of  $N$  observed). The final dataset consisted of 3,751 observations of  $r_{it}$  (SFig 1).

## Analysis

Bespoke models were constructed for all considered parameterisations of the travelling waves (summarised in Fig. 1 and Table 1), based on previous models of travelling waves (Lambin *et al.* 1998; Mosset *et al.* 2000; Berthier *et al.* 2014). All of the travelling wave models contained at least three components. The first component estimated distance from either a reference planar direction or an epicentre location (*Distance equation*, Table 1). The next used these distances and converted them to a space-modified time variable (*Space-modified time equation*, Table 1), itself then used in a GAM (generalised additive models) to explain growth rates (*Growth equation*, Table 1). These models reflect various ways to modify space and time so that the dynamics at each location can be explained by one or two underlying cycles (see Fig. 1). The parameters defining the space-modified time variables of the travelling waves were estimated using a stochastic annealing (SANN) optimiser (Bolker 2008), using 15,000 iterations for each model. SANN initial values were determined using a direct search method to crudely characterise the parameter space. Conditional on the values of the space-modified time variables, the underlying cycles were fitted using GAMs as described below.

Three versions of a "null" model (i.e., no travelling wave pattern) were included in the analysis and fit using generalised additive models alone. These included a true null model ( $N_1$ ), a model which assumed true synchrony ( $N_2$ ), and a final model which proposed growth rates were explained by space alone ( $N_3$ ) (Table 1).

All GAM components (*Growth equation*, Table 1) assumed a Normal distribution for random errors and included a weighting term. The weighting term was the square root of the differential in surveys from a centroid ( $\varpi_{t,i}$ ) =  $\sqrt{\frac{n_{t,i} \times n_{t-1,i}}{n_{t,i} + n_{t-1,i}}}$ , where  $\varpi_{t,i}$  is the weights for centroid  $i$  at time  $t$ , and  $n$  is the number of surveys in time  $t$  and  $t-1$ . The term sought to account for observation variance caused by the adaptive vole monitoring intensity, whereby the number of transects varied over time (transects per centroid ranged from 2 to 111, with a mean of 18.5). The appropriateness of the weight term was checked by plotting model residuals against the weighted term.

All bespoke models reflected either radial or planar waves parameterisations. Models P, RE and RC were the simplest and included either a single planar (P), expanding radial (RE), or contracting radial (RC) travelling wave. A further suite of models assumed the presence of two spatially isolated, i.e., non-interfering, waves separated by the Duero river, with the waves being either planar (PF), expanding radial (RFE), or contracting radial (RFC). The potential for a single pattern informed by dual additive, overlapping waves was captured by allowing models to have two waves, either planar (PD), expanding radial (RDE) or contracting radial (RDC) waves. Compared to the models with two waves isolated by a physical feature, these models assumed that both waves influenced all populations in the landscape. This suite of models represents various predicted forms of travelling waves and some logical extensions to ensure a number of candidate models are considered. Given the richness of our data, the panel of models considered extends previous research that has generally used a single form or descriptive methods that could not rule out competing hypotheses. Using this approach, we can quantitatively assess which description of the spatio-temporal patterns are most supported by our data.

Parameterisations of each travelling wave model are included in Table 1.

The final model was chosen based on parsimony considerations using  $\Delta AIC$  and the corresponding hypothesis selected over the alternatives (see supplementary material 1 for each model’s AIC values). AIC, as reported by the final GAM, was adjusted to incorporate the additional number of wave parameters as;

$$Adjusted\ AIC = AIC + 2K$$

where  $K$  is the number of wave parameters (table 1).

Confidence profiles for each parameter were determined using profiling as described in Bolker (2008). All analyses and visualisations were carried out in R version 4.0.2 (R core team 2020) using the *mgcv* (Wood 2011), *emdbook* (Bolker, 2020), *ggplot2* (Wickham 2016) and *patchwork* (Pedersen 2020) packages. The code used for the analysis is embedded in supplementary material 1.

To determine the statistical method’s effectiveness at retrieving known parameter values, we carried out a brief simulation study, available in supplementary material 2. Model assumption checks, residual plots, and summaries of each model are included in supplementary material 3.

## Results

The null models ( $N_1$ ,  $N_2$ , and  $N_3$ ) were discarded through model selection (see supplementary material 1), indicating that it is unlikely that there was true synchrony ( $N_2$ ), or that the observed growth rates are related to static environmental conditions ( $N_3$ ). The relative lack of support for  $N_2$  (true synchrony) provides evidence that large scale true synchrony is not the pattern characterising our dataset.

Of the models which assumed the presence of travelling waves, RDE (dual expanding radial travelling waves) was selected, with the next most parsimonious model (dual contracting radial, RDC) having  $\Delta AIC = 53.2$ . The final model had epicentres estimated 75.2 km apart (Fig. 2, Table 2). The first was in a well-known problematic area with higher-than-average vole abundances, with recurrent and severe outbreaks (*Tierra de Campos*). In contrast, the second was positioned further southeast, in an area that experiences lower than average abundances (see SFig. 2 for a  $G_1^*$  cluster analysis of the 42,973 abundance indices).

Additionally, when plotting the predicted growth rates on the space-modified time variables, the possibility that the overall pattern can be decomposed into possible activator and inhibitor influences (themselves, phenomenological statistical descriptions) on vole population growth is suggested; the first, slow wave predominantly inhibited growth and was estimated to travel radially at 148 km per year, while the second, faster wave was estimate to travel radially at 835 km per year and generally promoted growth (Fig. 3). When the effects of both of these waves are visualised over true space and time, the cumulative spatio-temporal pattern becomes apparent (Video 1) and the speed at which it traverses the region is approximately 0.9 km per day (or 329 km per year, calculated by extracting the furthest south predictions where  $r_t > 0.5$  [i.e., the wave front] at two arbitrarily chosen times, then calculating the distance between those and dividing by the difference in time).

## Discussion

We find clear evidence of a self-organising spatio-temporal pattern in the population growth rates of common voles in Castilla-y-León, resulting from two travelling waves spreading radially at contrasting speeds. Further, in line with Johnson *et al.* (2004), we find that the pattern in CyL is best approximated as two expanding radial travelling waves. However, the waves detected here are not independent as in Johnson *et al.* (2004), instead acting additively as activator and inhibitor, suggesting they may be more than phenomenological descriptions of an overall pattern. The dual expanding, fast and slow radial travelling waves, suggesting activator and inhibitor dynamics respectively, are of a form not previously observed in the empirical literature but are in line with the fundamental interactions of activators (e.g., host) and inhibitors (e.g., pathogens) in population cycles. Such activation and inhibition, and their spatial diffusion are similarly believed to be the

process generating synchrony (Vasseur & Fox 2009). Further, activator and inhibitor dynamics are inherently included in travelling wave simulations. As such, we find convergence between understandings of synchrony, travelling waves and population cycles.

### True synchrony or partial synchrony?

While we refer to the population cycle of common voles in CyL as partially synchronous, various studies have apparently demonstrated that cyclic populations, both of common voles and other cyclic species, occur synchronously. To understand this apparent contradiction, it is important to note that synchrony occurs, not as a dichotomous state but as a spectrum (Koenig 1999; Bjørnstad *et al.* 1999, see Fig. 1). Nevertheless, the dichotomous representation of synchrony has led to an approach whereby evidence of synchrony (notably synchrony which decays with distance) can be perceived as evidence, or lack-there-of, of true synchrony (Smith 1983; Andersson & Jonasson 1986; Erlinge *et al.* 1999; Huitu *et al.* 2003; Sundell *et al.* 2004; Lambin *et al.* 2006; Huitu *et al.* 2008; Fay *et al.* 2020;). The use of the terms “synchrony” and “asynchrony”, which implies a dichotomous state, may lead to the view that there are no nuanced forms of synchrony.

If travelling waves are ubiquitous in cyclic populations, a crucial component to detecting such nuanced forms of synchrony, overcome in the present study, is the requirement for a vast amount of data to distinguish between more subtle forms (Koenig 1999). Early descriptions of population cycle synchrony were largely limited to qualitative assessments, where populations were deemed synchronous if they peaked sometime in the same year (e.g., Andersson & Jonasson 1986). While such qualitative assessments of synchrony may reflect genuine true synchrony, they likely suffer from temporal aggregations, i.e., where population synchrony is deemed to have occurred because the same phase is experienced within the same broad period of time (see SFig. 3 for an example of where a travelling wave could be misconstrued as true synchrony using a qualitative approach). While research on synchrony has become more quantitative, some subsequent attempts to characterise synchrony have suffered from similar issues, namely, a lack of either or both spatial and temporal resolution (Koenig, 1999).

Perhaps owing to the long history of time series use in population cycle literature, many datasets which test for synchrony generally last for a long period of time (e.g., 21 years in Huitu *et al.* 2003). However, even in long term datasets, the temporal resolution can be severely limited. For instance, Sundell *et al.* (2004) used the annual breeding output of raptors in 50 km x 50 km areas across Finland, as a vole abundance index to characterise synchrony across the country. While such datasets are likely able to determine if true asynchrony or true synchrony are better supported (e.g., peaks occur in the same year), they seem ill-suited for detecting more subtle forms of synchrony as any signal of a within year spatio-temporal delay in synchrony (e.g., a travelling wave) would be obscured.

While such issues surrounding temporal resolution and aggregation may mask more subtle forms of synchrony, such as travelling waves, a lack of spatial resolution is perhaps equally detrimental. Indeed, in many instances, population synchrony has been characterised using far fewer spatial replicates than those used in this analysis (Huitu *et al.* 2003; Lambin *et al.* 2006; Huitu *et al.* 2008). In such cases of comparatively low spatial resolution, as with studies with a low temporal resolution, the result may be an ability to distinguish between the two extremes of synchrony but an inability to explore where a metapopulation exists on the spectrum of synchrony.

Indeed, whenever spatio-temporal datasets have been rich in both spatial and temporal resolution, the outcome appears to be the detection of travelling waves, irrespective of the method used (Lambin *et al.* 1998; Cummings *et al.* 2004; Johnson *et al.* 2004; Grenfell *et al.* 2013; Berthier *et al.* 2014). Such datasets tend to exist only for species with public health or economic interests, such as pest species (Bjørnstad 2001), which may, in part, explain the relatively few examples of travelling waves in the literature compared to detections of apparent true synchrony. However, if the waves captured here do represent activator-inhibitor dynamics and their dispersal, it is logical to assume that all cyclic systems are synchronised via travelling waves, which are only subsequently modified more or less by the Moran effect (Hugueny 2006).

### Activator-inhibitor waves

Given the long history of using activator-inhibitor systems to model population cycles (e.g., Levin 1974), as well as the finding that trophic interactions and dispersal promote synchrony, our findings, which suggest the presence of activator and inhibitor travelling waves, provide some measure of consistency between understandings of synchrony and population cycle theory (Bjørnstad 2001; Bierman *et al.* 2006). Such activator-inhibitor travelling waves have previously been detected in cellular biology (Kapustina *et al.* 2013; Martinet *et al.* 2017) but not in ecology.

Our results are, to our knowledge, the first instance where a single spatio-temporal pattern of population cycles has been decomposed into constituent parts, which we propose represent the influences of activator and inhibitor on population vole growth. Microcosm experiments investigating the effects of dispersal and trophic interactions (and the Moran effect) found that the synchronising effect of dispersal in the presence of predation led to greater synchrony in population cycles of protists (Vasseur & Fox 2009), suggesting that the two waves here may partly represent the synchronising effects of dispersal of voles, dispersal of inhibitors (possibly pathogens or predators) and the interactions between them. Indeed, a potential candidate agent for an inhibitor, pathogens, are known to spread via travelling waves (Grenfell *et al.* 2001; Cummings *et al.* 2004).

The presence of two epicentres is in line with previous research on travelling waves (Johnson *et al.* 2004), though the finding that final cumulative pattern is dependent on both epicentres, with apparently distinct roles (i.e., activation and inhibition of growth rates, Fig. 3) are new to the field. The positioning of the epicentres, estimated as distinct locations with no overlap in the 95% CI, may provide some support for the interpretation of activator and inhibitor dynamics. The estimated location of the inhibitor epicentre is in an area with higher-than-average abundances of voles (*Tierra de Campos*, see SFig. 2). This region is known locally to practitioners for recurrently experiencing severe outbreaks, which may be related to farming practices which are more suitable for voles (Roos *et al.* 2019). Such a location would present an area consistent with understandings of where travelling waves of diseases initiate, as pathogen travelling waves have been found to originate in areas of high density (Grenfell *et al.* 2001; Cummings *et al.* 2004). If so, this epicentre may represent the starting location for the outward spread of pathogens because of infected dispersing individuals which serve to inhibit growth rates of voles. A testable hypothesis would be that this region experiences a higher proportion of infected individuals compared to a regional average. Indeed, two pathogens, Tularemia and bartonella, are known to occur in a density dependent relationship with vole densities in *Tierra de Campos* (Rodríguez-Pastor *et al.* 2017). A consequence of being reliant on dispersers for the propagation of the disease, in combination with various delaying processes (e.g., latency to infection), is that we would expect that the speed of the inhibitor to be slower than the activator speed, which we observe (Table 2).

Conversely, the activator epicentre was located in a lower-than-average abundance region (see SFig. 2). We propose that this may be due to a slight adjustment to the epicentre hypothesis as described in Johnson *et al.* (2006). The epicentre hypothesis posits that emigration between close suitable habitats causes travelling waves. We consider that our epicentre meets these requirements in all but “suitable habitat” (i.e. lower-than-average densities). However, given the high reproductive capacity of common voles, we would assume they are able to produce as many offspring in a “less-suitable habitat” as elsewhere in the region, but that most of these offspring become emigrants. In this light, the core understanding of the epicentre hypothesis is maintained, where an epicentre is a location producing many emigrants, but altering it to take into account the reproductive ability of common voles which we do not believe has influential spatial variation. Evidence of this would come from finding a higher-than-average proportion of dispersers at this location.

The speed of the inhibitor wave was estimated at 147 km per year, while the activator was estimated at 835 km per year, which appear to be middle-ground speed estimates amongst empirical travelling wave literature (which vary from a minimum of 7-8 km per year [Berthier *et al.* 2014] to a maximal 1,776 km per year [Cummings *et al.* 2006]). Differences in speed offers some confirmation with simulations (Johnson *et al.* 2006), where differences in activator-inhibitor dispersal abilities was found to result in radial travelling waves. We propose that pathogen (i.e., a possible inhibitor) diffusion would be dependent on, host dispersal,

mode of transmission, latency to infection, and so forth, all possible means to impart a delay in the spread to adjoining populations. Conversely, we believe that the fast speed of the activator wave may reflect the relative ease at which voles are able to disperse (i.e., habitat connectivity, where CyL is criss-crossed by field margins) or the effectiveness of a dispersal event (related to density).

Our modelling has demonstrated evidence for both activator and inhibitor influences on population growth rates in voles. Further work is required to establish the processes underlying these influences, and to collect sufficient large-scale data on other ecological systems to establish whether these too are underpinned by activator and inhibitor influences.

## Acknowledgements

We are indebted to the staff of the Área de Plagas, Instituto Tecnológico Agrario de Castilla-y-León (ITACyL) and the Consejería de Agricultura, Ganadería y Desarrollo Rural de la Junta de Castilla-y-León, who collected the data within the ITACYL 2007/2155 Project and the Monitoring Program of common vole populations in Castilla-y-León. The analysis and DR were funded by Biotechnology and Biological Sciences Research Council (BBSRC) [grant number BB/M010996/1], through Eastbio DTP. The study contributes to the BOOMRAT project (MINECO: PID2019-109327RB-I00). We are grateful to Thomas Cornulier and Nigel Yoccoz who provided feedback as part of the PhD viva for DR.

## References

- Andersson, M. and Jonasson S., 1986. Rodent cycles in relation to food resources on an alpine heath. *Oikos*, 46, 93-106
- Andreassen, H.P. and Ims, R.A. (2001). Dispersal in patchy vole populations: role of patch configuration, density dependence, and demography. *Ecology*, 82(10), 2911-2926.
- Bailles, A., Collinet, C., Philippe, J.-M., Lenne, P.-F., Munro, E. and Lecuit, T. (2019). Genetic induction and mechanochemical propagation of a morphogenetic wave. *Nature*, 572(7770), 467-473.
- Banerjee, M., Ghorai, S. and Mukherjee, N. (2017). Approximated Spiral and Target Patterns in Bazykin's Prey-Predator Model: Multiscale Perturbation Analysis. *Int J Bifurcat Chaos*, 27(03), 1750038.
- Berthier, K., Piry, S., Cosson, J.-F., Giraudoux, P., Foltête, J.-C., Default, R., et al. (2013). Dispersal, landscape and travelling waves in cyclic vole populations. *Ecol Lett*, 17(1), 53-64.
- Berryman, A. et al. (2002). *Population cycles: the case for trophic interactions*. Oxford University Press.
- Bierman, S.M., Fairbairn, J.P., Petty, S.J., Elston, D.A., Tidhar, D. and Lambin, X. (2006). Changes over Time in the Spatiotemporal Dynamics of Cyclic Populations of Field Voles (*Microtus agrestis* L.). *Am Nat*, 167(4), 583-590.
- Bjørnstad, O.N. (2000). Cycles and synchrony: two historical "experiments" and one experience. *J Anim Ecol*, 69(5), 869-873.
- Bjørnstad, O.N. and Bascompte, J. (2001). Synchrony and Second-Order Spatial Correlation in Host-Parasitoid Systems. *J Anim Ecol*, 70(6), 924-933.
- Bjørnstad, O.N., Peltonen, M., Liebhold, A.M. and Baltensweiler, W. (2002). Waves of Larch Budmoth Outbreaks in the European Alps. *Science*, 298(5595), 1020-1023.
- Blasius, B., Huppert, A. and Stone, L. (1999). Complex dynamics and phase synchronization in spatially extended ecological systems. *Nature*, 399(6734), 354-359.
- Bolker, B.M. (2008). *Ecological Models and Data in R*. Princeton University Press.
- Bolker, B.M. (2020). *emdbook: Ecological Models and Data in R*, R package version 1.3.12.
- Bogdziewicz, M., Hackett-Pain, A., Ascoli, D. and Szymkowiak, J. (2021). Environmental variation drives continental-scale synchrony of European beech reproduction. *Ecology*, 03384.
- Bowler, D.E. and Benton, T.G. (2005). Causes and consequences of animal dispersal strategies: relating individual behaviour to spatial dynamics. *Biol Rev*, 80(2), 205-225.
- Bugrim, A.E., Dolnik, M., Zhabotinsky, A.M. and Epstein, I.R. (1996). Heterogeneous Sources of Target Patterns in Reaction-Diffusion Systems. *J Phys Chem*, 100(49), 19017-19022.
- Cummings, D.A.T., Irizarry, R.A., Huang, N.E., Endy, T.P., Nisalak, A., Ungchusak, K. et al. (2004). Travelling waves in the occurrence of dengue haemorrhagic fever in Thailand. *Nature*, 427(6972), 344-347.
- De Roos, A.M., McCauley, E. and Wilson, W.G. (1991). Mobility versus density-limited predator-prey dynamics on different spatial scales. *Proc Royal Soc B*, 246(1316), 117-122.
- Erlinge, S., Danell, K., Frodin, P., Hasselquist, D., Nilsson, P., Olofsson, E.B. et al. (1999). Asynchronous population dynamics of Siberian lemmings across the Palaearctic tundra. *Oecologia*, 119(4), 493-500.
- Fay, R., Michler, S., Laesser, J., Jeanmonod, J. and Schaub, M. (2020). Large-scale vole population synchrony in central Europe revealed by Kestrel breeding performance. *Front Ecol Evol*, 7, 512.
- Fox, J.W., Legault, G., Vasseur, D.A. and Einarson, J.A. (2013). Nonlinear Effect of Dispersal Rate on

Spatial Synchrony of Predator-Prey Cycles. *PLoS ONE*, 8(11), e79527. Garcia, J.T., Dominguez-Villasenor, J., Alda, F., Calero-Riestra, M., Perez Olea, P., Fargallo, J.A., *et al.* (2019). A complex scenario of glacial survival in Mediterranean and continental refugia of a temperate continental vole species (*Microtus arvalis*) in Europe. *J Zoolog Syst Evol*, 58(1), 459–474. Gibert, J.P. and Yeakel, J.D. (2019). Laplacian matrices and Turing bifurcations: revisiting Levin 1974 and the consequences of spatial structure and movement for ecological dynamics. *Theor Ecol*, 12(3), 265–281. Grenfell, B.T., Bjornstad, O.N. and Kappey, J. (2001). Travelling waves and spatial hierarchies in measles epidemics. *Nature*, 414(6865), 716–723. Gurney, W.S.C., Veitch, A.R., Cruickshank, I. and McGeachin, G. (1998). Circles and spirals: population persistence in a spatially explicit predator-prey model. *Ecology*, 79(7), 2516–2530. Hugueny, B. (2006). Spatial synchrony in population fluctuations: extending the Moran theorem to cope with spatially heterogeneous dynamics. *Oikos*, 115(1), 3–14. Jareno, D., Vinuela, J., Luque-Larena, J.J., Arroyo, L., Arroyo, B. and Mougeot, F. (2014). A comparison of methods for estimating common vole (*Microtus arvalis*) abundance in agricultural habitats. *Ecol Indic*, 36, 111–119. Jareno, D., Vinuela, J., Luque-Larena, J.J., Arroyo, L., Arroyo, B. and Mougeot, F. (2015). Factors associated with the colonization of agricultural areas by common voles *Microtus arvalis* in NW Spain. *Biol Invasions*, 17(8), 2315–2327. Jepsen, J.U., Vindstad, O.P.L., Barraquand, F., Ims, R.A. and Yoccoz, N.G. (2016). Continental-scale travelling waves in forest geometrids in Europe: an evaluation of the evidence. *J Anim Ecol*, 85(2), 385–390. Johnson, D.M., Bjornstad, O.N. and Liebhold, A.M. (2004). Landscape geometry and travelling waves in the larch budmoth. *Ecol Lett*, 7(10), 967–974. Johnson, D.M., Bjornstad, O.N. and Liebhold, A.M. (2006). Landscape Mosaic Induces Traveling Waves of Insect Outbreaks. *Oecologia*, 148(1), 51–60. Koenig, W.D. (1999). Spatial autocorrelation of ecological phenomena. *Trends Ecol Evol*, 14(1), 22–26. Huitu, O., Norrdahl, K. and Korpimäki, E. (2003). Landscape effects on temporal and spatial properties of vole population fluctuations. *Oecologia*, 135(2), 209–220. Huitu, O., Laaksonen, J., Klemola, T. and Korpimäki, E. (2008). Spatial dynamics of *Microtus* vole populations in continuous and fragmented agricultural landscapes. *Oecologia*, 155(1), 53–61. Ims, R.A. and Andreassen, H.P. (2005). Density-dependent dispersal and spatial population dynamics. *Proc Royal Soc B*, 272(1566), 913–918. Ims, R.A. and Hjernmann, D.O. (2001). Condition-dependent dispersal. In: *Dispersal* {eds. Clobert, J., Danchin E., Dhont, A.A., Nichols, J.D.} Oxford University Press, Oxford, pp. 203–216 Kapustina, M., Elston, T.C. and Jacobson, K. (2013). Compression and dilation of the membrane-cortex layer generates rapid changes in cell shape. *J Cell Biol*, 200(1), 95–108. Lambin, X., Elston, D.A., Petty, S.J. and MacKinnon, J.L. (1998). Spatial asynchrony and periodic travelling waves in cyclic populations of field voles. *Proc Royal Soc B*, 265(1405), 1491–1496. Lambin, X., Aars, J., Pieltney, S. (2001). Dispersal, intraspecific competition, kin competition and kin facilitation: a review of the empirical evidence. In: *Dispersal* {eds. Clobert, J., Danchin E., Dhont, A.A., Nichols, J.D.} Oxford University Press, Oxford, pp. 110–122 Lambin, X., Bretagnolle, V. and Yoccoz, N.G. (2006). Vole population cycles in northern and southern Europe: is there a need for different explanations for single pattern? *J Anim Ecol*, 75(2), 340–349. Levin, S.A. (1974). Dispersion and Population Interactions. *Am Nat*, 108(960), 207–228. Li, Z., Gao, M., Hui, C., Han, X. and Shi, H. (2005). Impact of predator pursuit and prey evasion on synchrony and spatial patterns in metapopulation. *Ecol Modell*, 185(2–4), 245–254. Liebhold, A., Koenig, W.D. and Bjornstad, O.N. (2004). Spatial Synchrony in Population Dynamics. *Annu Rev Ecol Evol Syst*, 35(1), 467–490. Pedersen T.L. (2020). patchwork: The Composer of Plots. <https://patchwork.data-imaginist.com>, <https://github.com/thomasps85/patchwork>. Luque-Larena, J.J., Mougeot, F., Vinuela, J., Jareno, D., Arroyo, L., Lambin, X. *et al.* (2013). Recent large-scale range expansion and outbreaks of the common vole (*Microtus arvalis*) in NW Spain. *Basic Appl Ecol*, 14(5), 432–441. Mackinnon, J.L., Petty, S.J., Elston, D.A., Thomas, C.J., Sherratt, T.N. and Lambin, X. (2001). Scale invariant spatio-temporal patterns of field vole density. *J Anim Ecol*, 70(1), 101–111. Maron, J.L. and Harrison, S. (1997). Spatial Pattern Formation in an Insect Host-Parasitoid System. *Science*, 278(5343), 1619–1621. Martinet, L.-E., Fiddymont, G., Madsen, J.R., Eskandar, E.N., Truccolo, W., Eden, U.T., *et al.* (2017). Human seizures couple across spatial scales through travelling wave dynamics. *Nat Commun*, 8(1), 14896. Moss, R., Elston, D.A. and Watson, A. (2000). Spatial asynchrony and demographic traveling waves during red grouse population cycles. *Ecology*, 81(4), 981–989. Mougeot, F., Lambin, X., Rodriguez-Pastor, R., Romairone, J. and Luque-Larena, J. (2019). Numerical response of a mammalian specialist predator to multiple prey dynamics in Mediterranean farmlands. *Ecology*, 100(9). Muller, S.C.,

Mair, T. and Steinbock, O. (1998). Traveling waves in yeast extract and in cultures of *Dictyostelium discoideum*. *Biophys Chem*, 72(1-2), 37–47. Oli, M.K. (2019). Population cycles in voles and lemmings: state of the science and future directions. *Mamm Rev*, 49(3), 226–239. Pedersen, E.J., Miller, D.L., Simpson, G.L. and Ross, N. (2019). Hierarchical generalized additive models in ecology: an introduction with mgcv. *PeerJ*, 7, e6876. Pinot, A., Barraquand, F., Tedesco, E., Lecoustre, V., Bretagnolle, V. and Gauffre, B. (2016). Density-dependent reproduction causes winter crashes in a common vole population. *Popul Ecol*, 58(3), 395–405. R Core Team (2020). R: A language and environment for statistical computing. R Foundation for Statistical Computing, Vienna, Austria. Rodriguez-Pastor, R., Escudero, R., Vidal, D., Mougeot, F., Arroyo, B., Lambin, X., *et al.* (2017). Density-dependent prevalence of *Francisella tularensis* in fluctuating vole populations, northwestern Spain. *Emerg Infect Dis*, 23(8), 1377. Rodriguez-Pastor, R., Escudero, R., Lambin, X., Vidal, M.D., Gil, H., Jado, I., *et al.* (2018). Zoonotic pathogens in fluctuating common vole (*Microtus arvalis*) populations: occurrence and dynamics. *Parasitology*, 146(3), 389–398. Roos D., Saldana C.C., Arroyo B., Mougeot F., Luque-Larena J.J., & Lambin X., 2019. Unintentional effects of environmentally-friendly farming practices: Arising conflicts between zero-tillage and a crop pest, the common vole (*Microtus arvalis*). *Agric Ecosyst Environ*, 272, 105-113 Royama, T. (1992). *Analytical population dynamics*. Springer, Dordrecht. Satake, A. and Iwasa, Y. (2002). Spatially limited pollen exchange and a long-range synchronization of trees. *Ecology*, 83(4), 993-1005. Sherratt, J.A., Eagan, B.T. and Lewis, M.A. (1997). Oscillations and chaos behind predator–prey invasion: mathematical artifact or ecological reality? *Philos Trans R Soc Lond, B, Biol Sci*, 352(1349), 21–38. Sherratt, T.N., Lambin, X., Petty, S.J., Mackinnon, J.L., Coles, C.F. and Thomas, C.J. (2000). Use of coupled oscillator models to understand synchrony and travelling waves in populations of the field vole *Microtus agrestis* in northern England. *J Appl Ecol*, 37(s1), 148–158. Sherratt, J.A. (2001). Periodic travelling waves in cyclic predator-prey systems. *Ecol Lett*, 4(1), 30–37. Sherratt, J.A., Lambin, X., Thomas, C.J. and Sherratt, T.N. (2002). Generation of periodic waves by landscape features in cyclic predator–prey systems. *Proc Royal Soc B*, 269(1489), 327–334. Sherratt, J.A. (2003). Periodic Travelling Wave Selection by Dirichlet Boundary Conditions in Oscillatory Reaction-Diffusion Systems. *SIAM J Appl Math*, 63(5), 1520–1538. Sherratt, J.A., Lambin, X. and Sherratt, T.N. (2003). The Effects of the Size and Shape of Landscape Features on the Formation of Traveling Waves in Cyclic Populations. *Am Nat*, 162(4), 503–513. Sherratt, J.A. and Smith, M.J. (2008). Periodic travelling waves in cyclic populations: field studies and reaction–diffusion models. *J R Soc Interface*, 5(22), 483–505. Sherratt, J.A. (2016). Invasion Generates Periodic Traveling Waves (Wavetrains) in Predator-Prey Models with Nonlocal Dispersal. *SIAM J Appl Math*, 76(1), 293–313. Smith, M.J. and Sherratt, J.A. (2007). The effects of unequal diffusion coefficients on periodic travelling waves in oscillatory reaction–diffusion systems. *Phys D: Nonlinear Phenom*, 236(2), 90–103. Sprugel, D.G. (1976). Dynamic structure of wave-regenerated *Abies balsamea* forests in the north-eastern United States. *J Ecol*, 889-911. Sutherland, W.J., Gill, J.A. and Norris, K. (2004). Density dependent dispersal: concepts, evidence, mechanisms and consequences. In: *Dispersal* {eds. Bullock, J.M., Kneward, R.E., Hails, R.} Blackwells, Oxford, pp. 134-151 Sundell, J., Huitu, O., Henttonen, H., Kaikusalo, A., Korpimäki, E., Pietiäinen, H., *et al.* (2004). Large-scale spatial dynamics of vole populations in Finland revealed by the breeding success of vole-eating avian predators. *J Anim Ecol*, 73(1), 167-178. Tedesco, P. and Hugué, B. (2006). Life history strategies affect climate based spatial synchrony in population dynamics of West African freshwater fishes. *Oikos*, 115(1), 117-127. Vasseur, D.A. and Fox, J.W. (2009). Phase-locking and environmental fluctuations generate synchrony in a predator–prey community. *Nature*, 460(7258), 1007–1010. Vindstad, O.P.L., Jepsen, J.U., Yoccoz, N.G., Bjørnstad, O.N., Mesquita, M. d. S. and Ims, R.A. (2019). Spatial synchrony in sub-arctic geometrid moth outbreaks reflects dispersal in larval and adult life cycle stages. *J Anim Ecol*, 88(8), 1134–1145. Wickham H. (2016). *ggplot2: Elegant Graphics for Data Analysis*. Springer-Verlag New York. Wood, S.N. (2011) Fast stable restricted maximum likelihood and marginal likelihood estimation of semiparametric generalized linear models. *J R Stat Soc Ser B*, 73(1), 3-36 Ydenberg, R.C. (1987). Nomadic Predators and Geographical Synchrony in Microtine Population Cycles. *Oikos*, 50(2), 270–272.

## Tables

Table 1: Summary of analysis including model label, hypothesis, and equations used to estimate distance,

space-modified time and growth rate. Where  $r_{t,i}$  is the log difference growth rate of centroid  $i$  at time  $t$ ,  $\alpha_1$  is the intercept term,  $\epsilon$  is the Normal distributed residual error,  $T$  is day since start of study,  $f$  is used to represent thin-plate smoothing splines with a maximum of 12 bases ( $f_1, f_2, f_{\text{North}}$ , and  $f_{\text{South}}$ ),  $f_p$  is a thin-plate tensor product with a maximum of ten bases in each dimension,  $X$  is the mean centred easting coordinate (UTM),  $Y$  is the mean centred northing coordinate (UTM),  $D$  is the distance of a centroid from either a planar angle or radial epicentre,  $\theta$  is the angle of a planar wave (radian),  $\rho$  is the space-modified time variable,  $\zeta$  is the constant speed of the wave,  $\gamma$  and  $\psi$  are the easting and northing coordinates of a radial wave epicentre (mean centred UTM),  $N$  and  $S$  denote north and south of the Duero river. The number of additional travelling wave parameters for each model are included.

	<b>Hypothesis</b>	<b>Distance equation</b>	<b>Spa</b>
$N_1$	Null	NA	NA
$N_2$	Phase-locked	NA	NA
$N_3$	Static spatial pattern	NA	NA
$RE$	Single expanding radial wave	$D_i = -\sqrt{(\gamma - X_i)^2 + (\psi - Y_i)^2}$	$\rho_{t,i}$
$RC$	Single contracting radial wave	$D_i = \sqrt{(\gamma - X_i)^2 + (\psi - Y_i)^2}$	$\rho_{t,i}$
$P$	Single planar wave	$D_i = \sin(\theta) X_i + \cos(\theta) Y_i$	$\rho_{t,i}$
$RFE$	Two expanding radial waves separated by river	$D_{N,i} = -\sqrt{(\gamma_N - X_i)^2 + (\psi_N - Y_i)^2}, \quad \text{if } Y_i \geq 5,068m$ $D_{S,i} = -\sqrt{(\gamma_S - X_i)^2 + (\psi_S - Y_i)^2}, \quad \text{if } Y_i < 5,068m$	$\rho_{N,t}$ $\rho_{S,t}$
$RDE$	Dual overlapping expanding radial waves	$D_{1,i} = -\sqrt{(\gamma_1 - X_i)^2 + (\psi_1 - Y_i)^2}$ $D_{2,i} = -\sqrt{(\gamma_2 - X_i)^2 + (\psi_2 - Y_i)^2}$	$\rho_{A,t}$ $\rho_{I,t}$
$RFC$	Two contracting radial waves separated by river	$D_{N,i} = \sqrt{(\gamma_N - X_i)^2 + (\psi_N - Y_i)^2}, \quad \text{if } Y_i \geq 5,068m$ $D_{S,i} = \sqrt{(\gamma_S - X_i)^2 + (\psi_S - Y_i)^2}, \quad \text{if } Y_i < 5,068m$	$\rho_{N,t}$ $\rho_{S,t}$
$RDC$	Dual overlapping contracting radial waves	$D_{1,i} = \sqrt{(\gamma_1 - X_i)^2 + (\psi_1 - Y_i)^2}$ $D_{2,i} = \sqrt{(\gamma_2 - X_i)^2 + (\psi_2 - Y_i)^2}$	$\rho_{1,t}$ $\rho_{2,t}$
$PF$	Two planar waves separated by river	$D_{N,i} = \sin(\theta_N) X_i + \cos(\theta_N) Y_i, \quad \text{if } Y_i \geq 5,068m$ $D_{S,i} = \sin(\theta_S) X_i + \cos(\theta_S) Y_i, \quad \text{if } Y_i < 5,068m$	$\rho_{N,t}$ $\rho_{S,t}$
$PD$	Dual overlapping planar waves	$D_{1,i} = \sin(\theta_1) X_i + \cos(\theta_1) Y_i$ $D_{2,i} = \sin(\theta_2) X_i + \cos(\theta_2) Y_i$	$\rho_{A,t}$ $\rho_{I,t}$

Table 2: Summary of RDE wave parameter estimates. Labels are as noted in Table 1.

	<b>Parameter</b>	<b>Parameter label</b>	<b>Estimate</b>	<b>Lower 95% CI</b>	<b>Upper 95% CI</b>	<b>Units</b>
1 <sup>st</sup> wave	Centroid (N)	$\gamma_1$	-41,723	-51,645	-33,626	UTM (mean centred)
	Centroid (E)	$\psi_1$	28,414	18,556	29,897	UTM (mean centred)
	Speed	$\zeta_1$	405	316	528	m per day

	Parameter	Parameter label	Estimate	Lower 95% CI	Upper 95% CI	Units
2 <sup>nd</sup> wave	Centroid (N)	$\gamma_2$	23,675	5,161	42,607	UTM (mean centred)
	Centroid (E)	$\psi_2$	-8,675	-21,536	11,351	UTM (mean centred)
	Speed	$\zeta_2$	2,287	1,783	2,941	m per day

## Figures

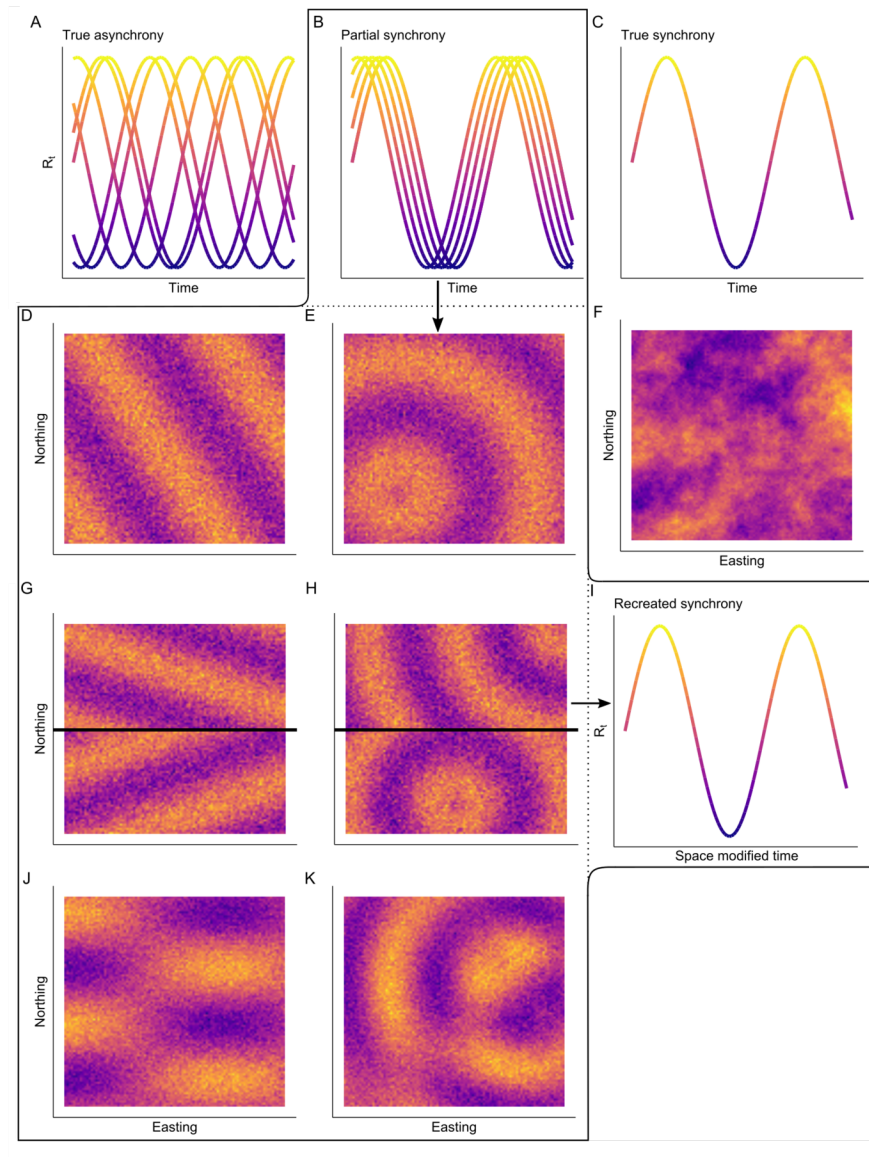


Figure 1: Visual representation of the various hypotheses (via simulated data), where yellow indicates high growth rates and blue low growth rates. **A** represents a truly asynchronous population cycle, where each population (line) cycles independently of its neighbours. **B** shows partial synchrony where the neighbouring populations' cycle almost simultaneously, though they are not perfectly synchronised (decomposed into subsequent models). **C** is a perfectly synchronised population where each population cycles at precisely the same time (where  $r_t$  should best be represented as varying with time, model  $N_2$ ). **F** shows a purely spatial pattern (where any perceived spatio-temporal pattern is merely spatial, model  $N_3$ , as Sherratt and Smith 2008 suggested may be the case for the apparent snowshoe hare travelling wave). **D** is a single planar wave at a snapshot in time (Moss *et al.* 2000; Lambin *et al.* 1998, Bjørnstad *et al.* 2002, Berthier *et al.* 2014, model P). **E** represents either an expanding or contracting single radial travelling wave (radially expanding from a central location as suggested by Johnson *et al.* 2006 [model RE] or contracting as suggested by Sherratt & Smith 2008, [model RC]). **G** shows two isolated planar waves separated by a physical feature, the Duero river (inferred from Sherratt & Smith 2008, model PF). **H** shows two radial waves separated by the same physical feature but may be either contracting or expanding (models RFE and RFC). **J** represents dual overlapping planar waves, which additively form a single overall pattern (model PD). **K** is either dual overlapping contracting or expanding radial waves, additively forming an overall pattern (models RDE and RDC). **I** represents the modelling approach, represented by the borders and arrows, used by the various parameterisations for each model, described in Table 1, to recreate a synchronised cycle in order to infer the form of partial asynchrony.

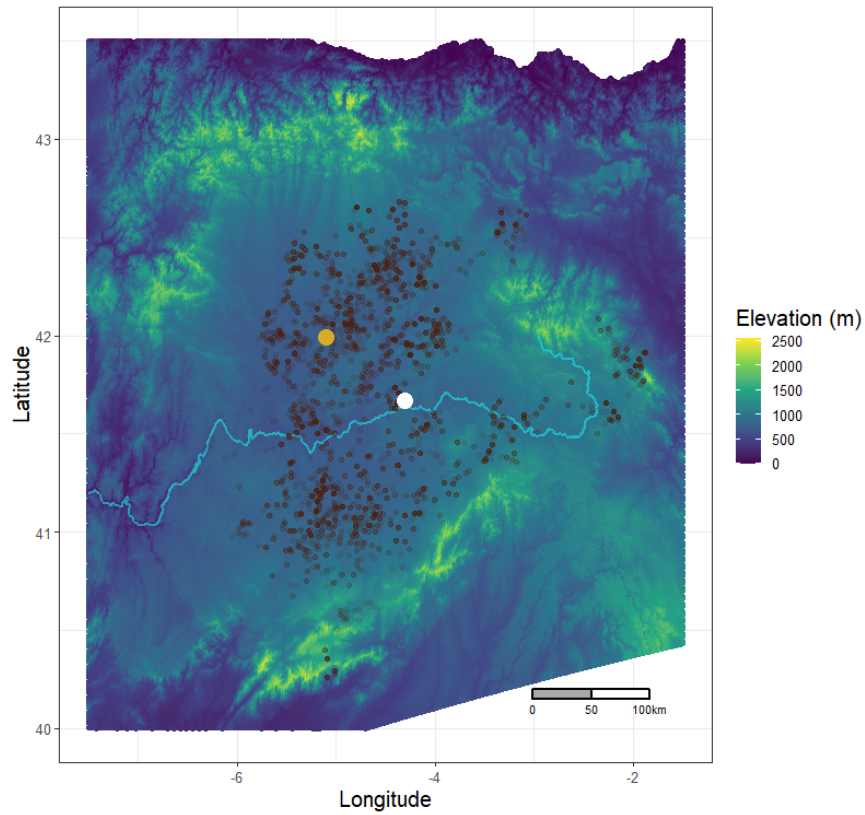


Figure 2: Map of the Duero basin, coloured according to elevation (m) with mountains in the north, east and south visible as bright yellow regions. The Bay of Biscay is visible in the north. Grey dots represent the sampling locations for population growth rates. Estimated epicentre locations are noted with the mustard

and white points. The Duero river is visible as the turquoise line running east to west. Elevation data was downloaded from copernicus[dot]eu (EU-DEM v1.1) and waterway data from ea[dot]europa[dot]eu.

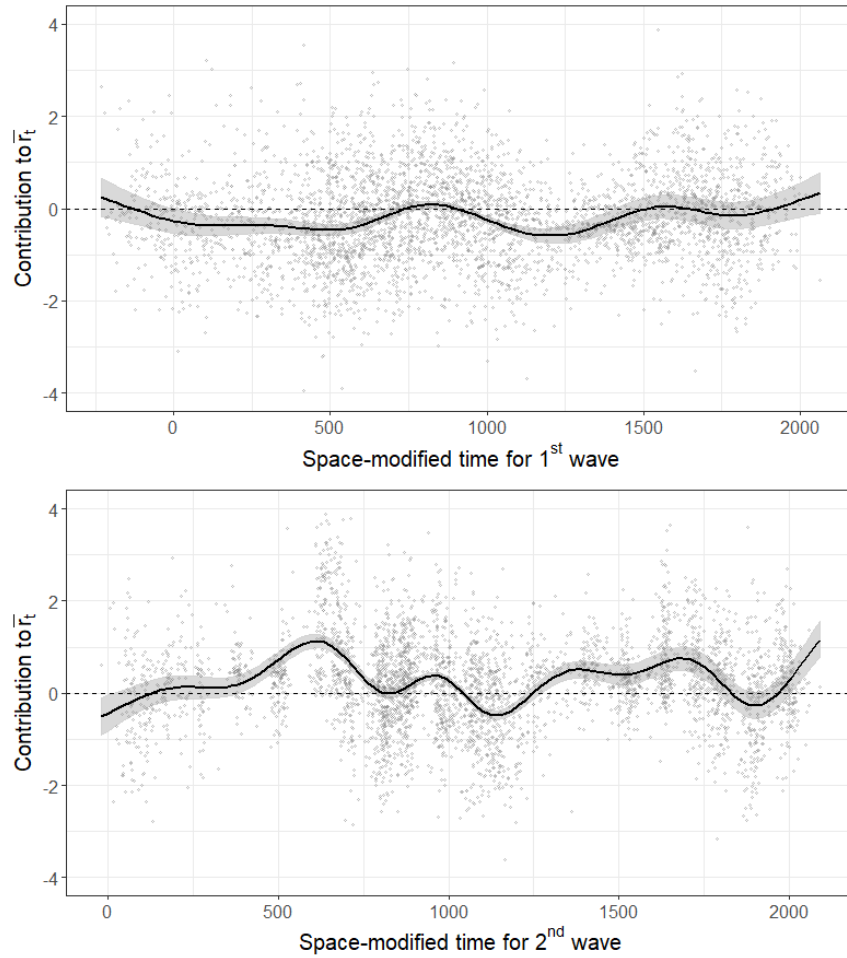


Figure 3: Conditional predictions, showing the contribution of the 1<sup>st</sup> (slow) and 2<sup>nd</sup> (fast) waves, including the intercept, to mean growth rate ( $r_{it}$ , y-axis) over space-modified time (x-axis) represented by the solid black lines, with 95% confidence intervals represented by the grey ribbons. Horizontal black dashed line indicates a growth rate of 0. The light grey points represent the partial residuals for the respective smoothing spline.

<Attached as separate file>

Video 1: Predicted underlying spatio-temporal pattern of  $r_{i,t}$  as a result of both travelling waves (model RDE), animated over true time (i.e., days since the start of the study).